Uncertainty quantification in 2D morphodynamic models

R. S. Mouradi
Saint-Venant Laboratory for Hydraulics
Email: remsophia.mouradi@gmail.com

C. Goeury
EDF R&D National Laboratory for Hydraulics and Environment (LNHE)

Y. Audoin
EDF R&D National Laboratory for Hydraulics and Environment (LNHE)

N. Claude
EDF R&D National Laboratory for Hydraulics and Environment (LNHE)

P. Tassi
EDF R&D National Laboratory for Hydraulics and Environment (LNHE)
Saint-Venant Laboratory for Hydraulics

K. El kadi Abderrezzak
EDF R&D National Laboratory for Hydraulics and Environment (LNHE)
Saint-Venant Laboratory for Hydraulics

August 23, 2017

Abstract

In this study, the modules TELEMAC-2D and SISYPHE of the Telemac-Mascaret Modelling System (TMS) have been used in combination with the OpenTURNS library (`www.openturns.org`) to perform an uncertainty quantification analysis of two-dimensional morphodynamic problems. OpenTURNS is a scientific library usable as a Python module dedicated to uncertainties treatment.

A recently implemented API (Application Program Interface) allowed the communication between OpenTURNS and TELEMAC-2D/SISYPHE, and therefore the efficient implementation of Monte-Carlo like algorithms. In this problem, each uncertain sedimentological parameter, e.g. inlet mean diameter, Shields parameter, etc. has been associated to a statistical distribution, defined with OpenTURNS. A number of TELEMAC-2D/SISYPHE simulations has been proposed regarding the pre-defined random entries in order to guarantee the convergence of the Monte Carlo-like algorithms.

This work allowed the implementation of uncertainty quantification analysis of computationally intensive morphodynamic simulations in the TMS. Thanks to the access to computer resources and optimized software, we were able to perform the uncertainty quantification analysis with a large set of variables, and therefore push the study further with the correlations effects analysis.

Keywords: Uncertainty quantification, Morphodynamic modelling, API, Monte-Carlo like algorithms, Sensitivity analysis

1 Introduction

Partie intro sujet

Morphodynamic simulations have been increasingly used in the last few decades to model the bed evolution in rivers, coasts and estuaries. In this context, most of the equations are empirical and the parameters involved in the calculations are generally poorly defined in literature. The impact of the uncertainties related to those parameters remains unknown.

In order to quantify the impact of inputs uncertainties on simulations results, an uncertainty study is conducted. Ranking the variables in terms of influence allows to orientate the investigations when performing measurements or calibrating parameters for the simulations. In this study, the uncertainty quantification is applied to SISYPHE [31], a sediments transport module, coupled with TELEMAC2D [26] for hydrodynamics, that integrate the TELEMAC-MASCARET modelling system.

Parler du calage effectué sur la partie hydrolique

blabla + ADAO

Parler incertitudes

The Monte Carlo method is used to propagate the uncertainties through SISYPHE. This approach requires random generation of several configurations of inputs, using their probability distributions. Successive deterministic model simulations are then submitted to generate a set of responses that correspond to the set of inputs.

Partie api

In order to have total control over the simulation's parameters and therefore conduct an efficient uncertainty study, an API (Application Program Interface) is developed for SISYPHE. This interface, when coupled with TELEMAC2D's available API, makes running hundreds of cases simultaneously possible through a cluster, taking total benefit from the available processors. Running an optimal number of cases guarantees the statistics convergence.

Finally, The pre-processing of uncertain data, as well as the post-processing of the results, are done using the OpenTURNS uncertainty library [2].

A ajouter : description biblio sur les incertitudes en sédimento

blabla

Organisation papier

This paper is organized as follows: a description of the context and general goals, followed by the present study objectives are given. Section 3 deals with the API's implementation and coupling with TELEMAC2D. Section 4 discusses the uncertainty quantification steps and alternates theory and results for each of these. In this section, a sensitivity analysis followed by an uncertainty propagation are investigated. Correlations between variables are also studied using copulas and an ANCOVA (ANalysis of COVAriance) sensitivity analysis is applied. In the last section, conclusions and perspectives are drawn.

2 Context and goals

This study is set out in the context of EDF numerical tools development. EDF's R&D National Laboratory for Hydraulics and Environment department (LNHE) uses the TELEMAC-MASCARET system to simulate complex hydro-environmental phenomenons (such as dam breaks and flooding risks) in order to anticipate the risks related to electrical production.

TELEMAC-MASCARET results are therefore expected to produce highly reliable results. However, a great number of parameters used in these studies, specifically in morphodynamic simulations, can be set by the user and are uncertain. In order to determine the uncertain parameters impact on the system's result, an uncertainty quantification study is necessary.

In this context, an uncertainty quantification study is conducted in the morphodynamic simulation module SISYPHE. To make this study possible, an API (Application Program Interface) is implemented and coupled to TELEMAC2D, to guarantee the inter-operability with SISYPHE.

3 API's development

The work here focused on the implementation of SISYPHE's API and its coupling to TELEMAC2D's already available API via FORTRAN modules. The API's main goal is to have control on a simulation while running a case. For example, it must allow the user to stop the simulation at any time step, retrieve some variables values and change them if necessary. SISYPHE's API is contained in the source folder of the TMS, as shown in Figure 1, and can therefore call all SISYPHE's subroutines to conduct morphodynamic simulations.

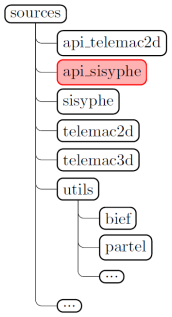

Figure 1: Extract of TELEMAC-MASCARET sources folders

In order to make this possible, a FORTRAN structure called instance was developed in the API. It contains a list of variables declared as pointers (memory addresses [12]) that are pointing to SISYPHE's variables. This gives direct access to the physical memory of variables, and allows therefore to retrieve their values, and modify them. Furthermore, modifications have been made in SISYPHE's main subroutines to make morphodynamic cases execution possible time step by time step. Finally, parallel runs have also been treated.

In addition to this, to make running coupled cases via the API possible, a communication interface is developed in FORTRAN. This interface contains communication subroutines that send TELEMAC2D's variables to SISYPHE and vice-versa. It also contains subroutines that manage coupled cases and take into consideration the coupling period.

A number of modifications in TELEMAC2D and SISYPHE sources were necessary. These modifications, along with the API and the coupling developments, were validated using three different compilers (NAG, IFORT, GFORTRAN), on classical SISYPHE cases and coupled TELEMAC2D-SISYPHE cases, available in the system.

Parler du wrapping Python

blabla

décrir le lien API-calage et API-incertitudes

4 Uncertainty quantification

4.1 Used Tool : Uncertainty treatment library OpenTURNS

OpenTURNS (Open source initiative to Treat Uncertainties, Risks'N Statistics) [2] is an open source C++ Library for uncertainty treatment used through python scripts. It is co-developed since 2005 by EADS IW, EDF R&D and PHIMECA Engineering. Various statistical methods are implemented in this library and allow to follow the uncertainty study steps [1] represented in Figure 2.

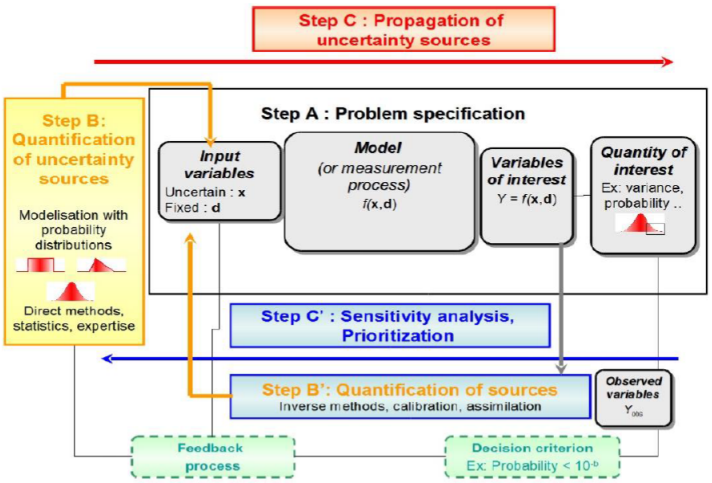

Figure 2: Steps for an uncertainty study

4.2 Uncertainty sources quantification

The goal here is to define variation intervals and probability density functions (PDF) for each uncertain parameters. We remind that, for a random variable X defined on an interval $[a, b]$, a PDF $f(x)$ is defined as follows :

$$\mathbb{P}(X \in [a, b]) = \int_a^b f(x)dx \tag{1}$$

For all the variables from 2 to 8 defined in Table **??**, variation intervals were found in literature, without further information about their probabilities. Consequently, using the principle of maximum entropy [4], uniform probability density functions are chosen for those variables.

For the experimental channel case, only one mean diameter measure is available and is subject to measurements errors. The errors interval is considered as a variation interval and a uniform PDF is applied for the mean diameter on its measurement interval. For the real bifurcation case, several samples of sediments are extracted in different sections of the river. Different values of the mean diameter are possible. In order to take all of them into consideration, a

PDF that corresponds to the sample is selected and validated via the QQ-Plot method [2].

4.3 Sensitivity analysis

4.3.1 Monte-Carlo Sampling and statistical estimations

The Monte Carlo method requires random generation of input variables from their probability distributions. The resulted sampling of a given size N is a $N \times V$ matrix, V being the number of uncertain parameters. Each row of the matrix $x^i = (x_1, ..., x_V)^i$ represents a possible configuration for the coupled hydro-morphodynamic simulation. Corresponding realizations of the output are generated by successive deterministic simulations with each configuration of the inputs. Statistical estimators of the response $Y = (Y_1, ..., Y_N) = (M(x^i))_{i \in \{1,...,N\}}$ can therefore be computed from the output as follows :

Mean :
$$E[Y] = \mu_Y = \frac{1}{N} \sum_{i=1}^{N} M(x^i) \tag{2}$$

Variance :
$$Var(Y) = \frac{1}{N-1} \sum_{i=1}^{N} [M(x^i) - \mu_Y]^2 \tag{3}$$

Standard deviation :
$$\sigma_Y = \sqrt{Var(Y)} \tag{4}$$

These statistical moments are useful for both the uncertainty sensitivity analysis and uncertainty propagation.

The convergence order of the Monte-Carlo sampling method is given by the Central Limit Theorem [10] as $\mathcal{O}\left(\frac{1}{\sqrt{N}}\right)$. The estimated statistics are also random quantities and are impacted by estimation uncertainties. Confidence intervals on estimators should therefore be calculated. The non-parametric "bootstrap" method provides information about the statistics uncertainties given few hypothesis [18]. Let $x = (x_1, ..., x_N)$ denote a sample of N independent and identically distributed realizations according to a probability density function $f(x)$. The statistical moment $\theta = T(F)$ (mean, variance, etc.), is estimated by $\hat{\theta} = T(\hat{F})$, where $\hat{F}$ is the empirical cumulative density function that gives equal probability $\frac{1}{N}$ to each observed value x_i defined by :

$$\hat{F}(x) = \frac{1}{d} \sum_{i=1}^{N} 1_{x_i \leq x} \tag{5}$$

The idea of the non-parametric bootstrap is to simulate data from the empirical cumulative density function. Given that $\hat{F}$ is build upon equal probability for the observations $(x_1, ..., x_N)$, a sample of same size N from $\hat{F}$ would simply be a selection from $(x_1, ..., x_N)$ with repeated values. A number of B samples are generated following this strategy, and estimators properties can therefore be deduced as shown in Figure 3.

The confidence interval I_θ is then estimated as follows :

$$I_\theta = [0.025 - q_{\widehat{\theta}_b}, 0.975 - q_{\widehat{\theta}_b}] \tag{6}$$

Where $\alpha - q_X$ is the α-quantile of a variable X defined as :

$$\mathbb{P}(X \leq q_X(\alpha)) = \alpha \quad \forall \alpha \in [0, 1] \tag{7}$$

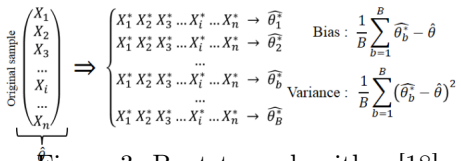

Figure 3: Bootstrap algorithm [18]

4.3.2 Analysis of variance

The main goal of a sensitivity analysis is to rank the uncertain parameters according to their influence. In order to do so, a definition of ranking indices is necessary. The indices used here are called Sobol Indices [17].

The definition of Sobol Indices is a result of the ANOVA (Analysis Of VAriance) variance decomposition. In fact, given a set of V **independent** uncertain parameters $X = (X_1, ..., X_V)$, the variance of a response $Y = M(X)$ can be calculated, using the total variance theorem [5], as follows [17]:

$$Var[Y] = \sum_{i=1}^{V} \mathcal{V}_i(Y) + \sum_{i<j} \mathcal{V}_{ij}(Y) + ... + \mathcal{V}_{12..V}(Y) \tag{8}$$

Where $\mathcal{V}_i(Y) = Var[E(Y|X_i)]$ and $\mathcal{V}_{ij}(Y) = Var[E(Y|X_iX_j)] - \mathcal{V}_i(Y) - \mathcal{V}_j(Y)$, etc.
$E(Y|X_i)$ is Y's conditional expectation with the condition that X_i remains constant.

One can therefore calculate first order sensitivity indices that estimate the influence of a variable X_i without its interactions with other variables:

$$S_i = \frac{\mathcal{V}_i(Y)}{Var[Y]} = \frac{Var(E[Y|X_i])}{Var[Y]} \tag{9}$$

And total indices that estimate the global influence of a variable (including interactions):

$$S_{Ti} = S_i + \sum_{j \neq i} S_{ij} + \sum_{j \neq i, k \neq i, j<k} S_{ijk} + ... = 1 - \frac{\mathcal{V}_{-i}(Y)}{Var[Y]} \tag{10}$$

$\mathcal{V}_{-i}(Y)$ being conditional expectations variances that do not involve X_i.

4.3.3 Numerical estimation of indices

There are two ways to estimate the Sobol indices defined in equations 9 and 10 :

SALTELLI method [10]: Step 1: Two independent samples A and B of size N are generated for the V uncertain variables. For example, sample A can

be written as follows:

$$A = \begin{pmatrix} x_1^{A,1} & x_2^{A,1} & ... & x_V^{A,1} \\ x_1^{A,2} & x_2^{A,2} & ... & x_V^{A,2} \\ \vdots & \vdots & \ddots & \vdots \\ x_1^{A,N} & x_2^{A,N} & ... & x_V^{A,N} \end{pmatrix} \tag{11}$$

A new sample C is created using columns of B except for column i that is replaced with data from A:

$$C = \begin{pmatrix} x_1^{B,1} & ... & x_i^{A,1} & ... & x_V^{B,1} \\ x_1^{B,2} & ... & x_i^{A,2} & ... & x_V^{B,2} \\ \vdots & & \vdots & & \vdots \\ x_1^{B,N} & ... & x_i^{A,N} & ... & x_V^{B,N} \end{pmatrix} \tag{12}$$

Simulations using the samples A, B and C result with :

$$\begin{cases} y_k^A = M((x_1^{A,k}, ..., x_V^{A,k})) & k = \{1, N\} \\ y_k^B = M((x_1^{B,k}, ..., x_V^{B,k})) & k = \{1, N\} \\ y_k^C = M((x_1^{C,k}, ..., x_V^{C,k})) & k = \{1, N\} \end{cases} \tag{13}$$

Which can be used to estimate Sobol indices as follows:

$$S_i = \frac{\frac{1}{N}\sum_{k=1}^{N} y_k^A y_k^C - (\mu_{Y^A})^2}{\sigma_{Y^A}^2} \tag{14}$$

$$S_{Ti} = 1 - \frac{\frac{1}{N}\sum_{k=1}^{N} y_k^B y_k^C - (\mu_{Y^B})^2}{\sigma_{Y^B}^2} \tag{15}$$

Overall, for a given sample size N, $(V + 2) \times N$ simulations are necessary to estimate the first order and total Sobol indices for each variable X_i.

Bootstrap on Saltelli estimation of Sobol indices :

Polynomial chaos method (PCE): The models response can be approached by an analytical function :

$$\begin{aligned} M(X) = M_0 + \sum_{i=1}^{V} M_i(X_i) + \sum_{1 \le i < j \le V} M_{i,j}(X_i, X_j) \\ + \quad ... \quad + M_{1,...,V}(X_1, ..., X_V) \end{aligned} \tag{16}$$

$M_i(X_i)$ represents the variable X_i's contribution to the result of the simulation. The variance can therefore be calculated as follows [5]:

$$\begin{aligned} Var[Y] = \sum_{u \subseteq \{1,...,V\}} [Var[M_u(X_u)] + \\ \sum_{v \subseteq \{1,...,V\}, v \cap u = \emptyset} Cov\left[M_v(X_v), M_u(X_u)\right]] \end{aligned} \tag{17}$$

In this particular case of independent variables, the covariance term $Cov\left[M_v(X_v), M_u(X_u)\right]$ vanishes, and the decomposition becomes then equal to ANOVA. Sobol indices can therefore be estimated as:

$$S_i = \frac{Var\left[M_i(X_i)\right]}{Var[Y]} \tag{18}$$

$$S_{Ti} = \frac{\sum_{u \subseteq \{1,\dots,V\}, i \in u} Var\left[M_u(X_u)\right]}{Var[Y]} \tag{19}$$

The contributions $M_i(X_i)$ can be calculated by estimating the models response using a polynomial chaos expansion, which can, in a simplified way, be written as:

$$M(X) = \sum_{|\alpha| \leq P} a_\alpha \Psi_\alpha(X) \tag{20}$$

Where $\{\Psi_\alpha, \alpha \in \mathbb{N}^V\}$ is a multivariate polynomial basis and a_α adequate coefficients for the estimation of the model's response, that can be determined using projection methods [5].

The X_i-univariate polynomials shares are the exact contribution of X_i to the polynomial expansion, and are therefore an estimation of $M_i(X_i)$.

Bootstrap on Polynomial chaos calculation of Sobol indices :

4.3.4 Results

4.4 Uncertainty propagation

In this section, the impact of the parameters uncertainty on the model's response will be investigated using statistics defined in section 4.3.1, like the mean and the variance.

To quantify the uncertainty propagation, a statistical number called variation coefficient is defined in equation 21.

$$c_v(Z_f) = \left| \frac{\sqrt{Var(Z_f)}}{\mu(Z_f)} \right| = \left| \frac{\sigma(Z_f)}{\mu(Z_f)} \right| \tag{21}$$

4.4.1 Results

Variation coefficients c_v are evaluated in interest points..

4.5 Correlations impact

Several physical relationships can exist between the considered uncertain parameters. These correlations between the variables can impact the uncertainty study, given that the parameters are no longer sampled independently. In order to model the correlations, copulas are introduced in section 4.5.1. For the sensitivity study, the ANOVA method can no longer be used, because of the independent parameters hypothesis it implies. A new method called ANCOVA (ANalysis of COVAriance) is introduced in section 4.5.2. The uncertainty study is conducted with the correlations consideration on the channel's case. In fact, given that the only influencing parameter in the Bifurcation is the diameter, it has been concluded that the correlation study for this case would be useless.

4.5.1 Copulas for correlations modelling

A copula is a function that defines a dependency structure between a set of variables [7]. In fact, it links the multivariate probability density function of random set of variables $(X_1, ..., X_V)$ to their univariate probability density functions.

A copula is a V-dimensional function C defined on $[0,1]^V$ that verifies:

- $\forall u \in [0,1]^V \ \forall i \in [|1:V|]$, if $u_i = 0$ then $C(u) = 0$
- $\forall i \in [|1:V|]$ and $u_i \in [0,1]$, $C(1, ..., 1, u_i, 1, ..., 1) = u_i$
- $\forall u, v \in [0,1]^V$ verifying $\forall i \in [|1:V|] \quad u_i \leq v_i$ then $V_C([u,v]) \geq 0$

Where $V_C([u,v])$ is the C-volume of the space $[u_1, v_1] \otimes \ldots \otimes [u_V, v_V]$ defined as follows :

$$V_C([u,v]) = \Delta_{u_V}^{v_V} ... \Delta_{u_1}^{v_1} C(\mathbf{w})$$

$\Delta_{u_i}^{v_i}$ being the i^{th} finite differential:

$$\begin{aligned} \Delta_{u_i}^{v_i} C(\mathbf{w}) = & C(w_1, ...w_i, v_i, w_{i+1}, ..., w_V) \\ & - C(w_1, ...w_i, u_i, w_{i+1}, ..., w_V) \end{aligned}$$

The Sklar theorem [7] allows to define a relation between the multivariate PDF f_X of the set $X = (X_1, ..., X_V)$ and the univariate probability density functions f_i of X_i as follows :

$$f_X(x_1, ..., x_V) = c(F_1(x_1), ..., F_V(x_V)) \times \prod_{i=1}^{V} f_i(x_i) \tag{22}$$

Where F_i are the univariate cumulative distribution functions of X_i associated to the probability density functions f_i. On the other hand, c is the probability density function of the copula C defined as follows:

$$\forall \mathbf{u} \in [0,1]^V \quad c(u_1, ..., u_V) = \frac{\partial^V C}{\partial u_1 ... \partial u_V}(u_1, ..., u_V) \tag{23}$$

In this study, a classical Gaussian copula is used [2]. It requires the calculation of a correlation Matrix using Spearman indices [2] from the relationships between variables. The relationships modelled here are the following:

- The modified Komura porosity formula [34]:

$$\lambda = 0.13 + \frac{0.21}{(d + 0.002)^{0.21}} \tag{24}$$

- The following relationship between the deviation parameter and the sediments diameter [21]:

$$\beta_2 = 9 \left(\frac{d}{H} \right)^{0.3} \tag{25}$$

4.5.2 Analysis of covariance

For dependent variables, it is possible to calculate the variance with the ANCOVA decomposition as follows:

$$\begin{aligned} Var[Y] = & \sum_{u \subseteq \{1,\dots,V\}} [Var[M_u(X_u)] \\ + & \sum_{v \subseteq \{1,\dots,V\}, v \cap u = \emptyset} Cov\left[M_v(X_v), M_u(X_u)\right]] \end{aligned} \tag{26}$$

New sensitivity indices can be defined as:

$$\begin{cases} S_i^U = \dfrac{Var\left[M_i(X_i)\right]}{Var[Y]} \\ S_i^C = \dfrac{Cov\left[M_i(X_i), \sum_{v \subseteq \{1,\dots,V\}, v \cap \{i\} = \emptyset} M_v(X_v)\right]}{Var[Y]} \\ S_i = S_i^U + S_i^C = \dfrac{Cov\left[M_i(X_i), Y\right]}{Var[Y]} \end{cases} \tag{27}$$

Where S_i is the total influence of the variable X_i, S_i^U the uncorrelated part of influence and S_i^C the correlated part.

ANCOVA indices can be negative because of the covariance term. In order to interpret the signification of negative indices, their absolute values are compared. In fact, if $|S_i^C|$ has a high value, this means that S_i^U is close to S_i, which signifies that correlations of the variable X_i have weak influence on the result. Inversely, if it has a high value, this means that correlations of X_i have great impact on the simulation's result.

Lastly, as show in section 4.3.2, the terms $M_i(X_i)$ can be estimated via the polynomial chaos expansion. However, in order to guarantee the orthogonality of the polynomial chaos basis, it is necessary to estimate the coefficients of the expansion using uncorrelated entries X. The M_i terms are estimated afterwards using the correlated values of the entries.

4.5.3 Results

The ANCOVA indices are compared to the Sobol (ANOVA) ones in order to quantify the impact of correlations on the sensitivity analysis, as shown in Figure

5 Application to morphodynamics processes

5.1 Governing equations

In this work, morphodynamics processes are considered by solving the depth-averaged hydrodynamics and bed evolution equations. The hydrodynamics equations are the shallow water or Saint-Venant equations (SWE) [20], expressed as:

$$\begin{cases} \dfrac{\partial h}{\partial t} + \nabla \cdot (\mathbf{u}h) = 0 \\ \dfrac{\partial \mathbf{u}}{\partial t} + \mathbf{u} \cdot \nabla \mathbf{u} + \nabla h = -g \nabla z_b - \dfrac{\boldsymbol{\tau}_b}{\rho h} + \dfrac{1}{h} \nabla \cdot (h \nu_t \nabla \mathbf{u}) \end{cases} \tag{28}$$

where $\mathbf{u}$ is the depth-averaged velocity vector with components (u, v) in the (x, y) horizontal directions; t is the time; h is the total water depth; z_b is the elevation of the bottom topography above datum, measured along the vertical coordinate z, and aligned against the direction of the acceleration of gravity of magnitude g; and ρ is the fluid density. To close the system (28), two additional relationships must be specified: (i) the shear stress vector $\boldsymbol{\tau}_b$ acting on the bed with components (τ_{b_x}, τ_{b_y}) in the (x, y) horizontal directions, and (ii) the depth-averaged turbulent eddy viscosity ν_t. For the former, the classical squared function dependency on the depth-averaged velocity is used:

$$\boldsymbol{\tau}_b = \rho C_f |\mathbf{u}| \mathbf{u}, \quad \text{with } |\mathbf{u}| = (u^2 + v^2)^{1/2}, \tag{29}$$

where the friction coefficient due to form drag plus skin friction $C_f = (u_*/|\mathbf{u}|)^2$ is specified with the relation:

$$C_f = g K^{-2} h^{-1/3}, \tag{30}$$

where K represents the Manning-Strickler roughness coefficient. Above, u_* denotes the shear velocity, defined by $u_* = \sqrt{|\boldsymbol{\tau}_b|/\rho}$, with $|\boldsymbol{\tau}_b| = (\tau_{b_x}^2 + \tau_{b_y}^2)^{1/2}$. For the latter, a constant depth-averaged eddy viscosity ν_t is adopted for this work. Appropriate initial and boundary conditions are specified to the system (28).

The bed evolution is accounted by solving a sediment mass balance or Exner equation. If only bed load transport is considered, the following equation arises [9]:

$$(1 - \lambda) \frac{\partial z_b}{\partial t} + \nabla \cdot \mathbf{q}_b = 0, \tag{31}$$

with λ the porosity and $\mathbf{q}_b$ the vector of volumetric transport rate per unit width without pores (m^2/s), with components q_{b_x}, q_{b_y} respectively in the x and y directions, such as:

$$\mathbf{q}_b = (q_{b_x}, q_{b_y}) = (q_b \cos\alpha, q_b \sin\alpha). \tag{32}$$

Above, q_b is the bedload transport rate per unit width, computed as a function of the equilibrium sediment load closure (or sediment transport capacity) and α is

the angle between the sediment transport vector and the downstream direction ($x-$axis). The dimensionless sediment transport rate Φ_b is expressed by:

$$\Phi_b = \frac{q_b}{\sqrt{g(s-1)d^3}}, \tag{33}$$

with $s = \rho_s/\rho$ the relative density $(-)$; ρ_s the sediment density (kg/m^3); ρ the water density (kg/m^3); and d the sand grain diameter, equal to the mean grain diameter d_{50} for uniform sediment distribution (m). Bed load transport formulas are generally computed as function of the non-dimensional shear stress or Shields parameter θ:

$$\theta = \frac{\mu|\boldsymbol{\tau}_b|}{(\rho_s-\rho)gd}, \tag{34}$$

with μ the correction factor for skin friction, computed as:

$$\mu = \frac{C'_f}{C_f} \tag{35}$$

where C'_f is the friction coefficient due only to skin friction, which is computed as:

$$C'_f = 2\left(\frac{\kappa}{\log(12h/k'_s)}\right)^2, \tag{36}$$

where κ is the von Kármán coefficient ($= 0.40$), the roughness height $k'_s = \alpha_{k_s} \times d_{50}$, the coefficient α_{k_s} is a calibration parameter.

The angle α is the angle between the sediment transport direction and the $x-$axis direction will deviate from that of the shear stress by combined action of a transverse slope and secondary currents. In a Cartesian coordinate system, this effect is incorporated in the formula [29]:

$$\tan\alpha = \frac{\sin\delta - \frac{1}{f(\theta)}\frac{\partial z_b}{\partial y}}{\cos\delta - \frac{1}{f(\theta)}\frac{\partial z_b}{\partial x}}. \tag{37}$$

Above, the terms $\partial z_b/\partial x$ and $\partial z_b/\partial y$ represent respectively the transverse and longitudinal slopes, and δ is the angle between the sediment transport vector and the flow direction, that can be modified by spiral flow. As in this work spiral flows are not considered, then $\delta = \tan^{-1}(v/u)$. The sediment shape function $f(\theta)$ is a function weighting the influence of the transverse bed slope, expressed as a function of the Shields parameter θ. It can be computed according to Talmon *et al.* [3] as $f(\theta) = 1/\beta_2\sqrt{\theta}$, with β_2 an empirical coefficient.

The correction of the magnitude of the sediment transport proposed by Soulsby [25] is based on the modification of the critical Shields parameter and is therefore only valid for threshold bedload formulas:

$$\frac{\theta^*_{cr}}{\theta_{cr}} = \frac{\cos\psi\sin\chi + \sqrt{\cos^2\chi\tan^2\phi - \sin^2\psi\sin^2\chi}}{\tan\phi}$$

where θ^*_{cr} is the corrected critical Shields number for a sloping bed, θ_{cr} is the critical Shields number for a flat, horizontal bed, ϕ is the angle of repose of the sediment, χ is the bed slope angle with the horizontal, and ψ is the angle between the flow and the bed slope directions.

In this work, two different sediment transport formulas used in many morphodynamic models are considered: the Meyer-Peter and Muller (MPM) formula [9, 22], which is a classical threshold formula that relates the bed load transport rate with the shear stress and the Grass formula [11], which is a continuous formula that relates the bed load to the flow velocities, based on the fact that some particle movement must occur at all nonzero time-mean velocities [6, 8, 14, 15].

The MPM formula is based on the grain mouvement threshold concept [9,22] and has a wide application range $d = d_{50} = [0.4 - 29]$mm. The dimensionless sediment transport rate is given by:

$$\Phi_b = \begin{cases} 0 & \text{if } \theta < \theta^*_{cr} \\ \alpha_{mpm}(\theta - \theta^*_{cr})^{3/2} & \text{otherwise} \end{cases} \tag{38}$$

with α_{mpm} a coefficient. A value of $\alpha_{mpm} = 8$ was proposed for the original MPM formula [9, 22].

The Grass formula is a simple power-law form of transport for non-cohesive sediment of uniform grain size [11]:

$$\Phi_b = \frac{\alpha_g}{\sqrt{g(s-1)d^3}} |\mathbf{u}|^{\beta_g}, \tag{39}$$

where α_g is a non-negative constant and $\beta_g = 3$.

5.2 Study cases : ANSWER

This case is a numerical reproduction of IRSTEA's laboratory experiment [33]
Description.
Décrire le cas d'étude ANSWER
- Lien avec la réalité (canaux de navigation?)
- Cas Labo –> Renvoyer vers article IRSTEA (information à obtenir)
- Observations qualitatives
- Phénomènes en jeu

Implémentation dans TELEMAC
Numerical case

5.3 Calage

Calage partie hydro
- Théorie
- ADAO

- Résultats coucou git

5.4 Range of the uncertain parameters

From the governing equations introduced in Section 5.1, the different parameters selected to perform the uncertainty analysis introduced in Section **??** are presented in Table 1. A uniform distribution is adopted based on the assumption that ... CEDRIC, SOPHIA A COMPLETER AVEC DEFINITION RIGUREUSE. As a guideline, the variability range of the values commonly found in the literature are presented in Table 1.

The variability mean sediment diameter is related to the source of uncertainty in measuring this quantity, which is estimated to the order of A POSER LA QUESTION A CELINE.

The limits of the range of variation associated with α_{mpm} (Equation 38) are equivalent to those proposed by Hunziker and Jaeggi [16] and Nielsen [24]. The variation of this coefficient can also be interpreted as if different sediment transport formulas are used as they are generally known to give results that can vary by more than one order of magnitude [27].

Although the coefficient α_g (Equation 39) can take values between 0 and 1 [8], most of the values found in the literature are in the range presented in Table 1. A value of α_g close to zero means a weak interaction between the sediment and the fluid.

Variables	Definitions	Units	Range	References
d_{50}	Sediment mean diameter	(m)	$[1.0,2.0]\times10^{-3}$	–
α_{mpm}	MPM's sediment transport coefficient	(-)	[5.0,12.0]	[16, 24]
α_g	Grass's sediment transport coefficient	(-)	$[1.0\times10^{-6},0.00167]$	[23, 28]
λ	Porosity	(-)	[0.25,0.40]	[9]
α_{k_s}	Skin friction coefficient	(-)	[1.0,6.6]	[13, 19]
ϕ	Angle of repose of the sediments (slope effect on sediment transport direction)	(°)	[28.0,46.0]	[32]
β_2	Deviation parameter (slope effect on sediment transport magnitude)	(-)	[0.20,1.90]	[30, 35]

Table 1: Uncertain parameters used in this work.

Decrire les intervalles de tous ces paramètres : Recherche faite par Nicolas

et Pablo

6 Conclusion and perspectives

In this study, an uncertainty quantification of a morphodynamic problem has been proposed.

In a sensitivity analysis step, differences were observed between a real case and an experimental case. In fact, for the real bifurcation case, the diameter was the only influencing parameter, which is not the same for the channel.

In order to analyse the influence of sediments diameter on the model's response, an uncertainty propagation study was conducted, considering as an only uncertain parameter the sediments diameter. This study has shown that the diameter has highly propagated uncertainties where there is movement. In fact, high variances were observed in maximum erosion points for the channel, and in a deposition zone for the bifurcation.

Finally, correlations were added and increased the variances significantly. An ANCOVA method was implemented in order to conduct a sensitivity analysis. The gap between the variables' influences decreased and variables that seemed first none-influencing (sediments diameter and transport coefficient of the Meyer-Peter and Müller formula) became of considerable influence when adding correlations.

This study can be generalized to other applications, such as the use of different sediment transport formulas, the study of suspended sediment transport or the influence of different physical phenomenons, for example waves (TOMAWAC module in the TELEMAC-MASCARET system).

References

[1] A. PASANISI, M. COUPLET and A.H DUTFOY LEBRUN, "Guide méthodologique pour le Traitement des Incertitudes," *Note EDF-MRI, reference H-T57-2013-02207-FR*, 2013.

[2] Airbus-EDF-IMACS-Phimeca, "Reference Guide - OpenTurns 1.7," 2016.

[3] T. A.M., S. N., and van Mierlo M.C.L.M, "Laboratory measurements of the direction of sediment transport on transverse alluvial-bed slopes." *J. of Hydr. Res.*, vol. 33(4), pp. 495–517, 1995.

[4] B. SUDRET, "Uncertainty propagation and sensitivity analysis in mechanical models. Contributions to structural reliability and stochastic spectral methods," *Accreditation to supervise research report*, 2007.

[5] Y. CANIOU, "Global sensitivity analysis for nested and multiscale modelling. PhD thesis. Blaise Pascal University Clermont II France," 2012.

[6] Z. Cao, R. Day, and S. Egashira, "Coupled and decoupled numerical modeling of flow and morphological evolution in alluvial rivers," *Journal of Hydraulic Engineering*, vol. 128, no. 3, pp. 306–321, 2002.

[7] G. CHASTAING, "Indices de Sobol généralisés pour variables dépendantes," 2010.

[8] M. C. Díaz, E. D. Fernández-Nieto, and A. Ferreiro, "Sediment transport models in shallow water equations and numerical approach by high order finite volume methods," *Computers & Fluids*, vol. 37, no. 3, pp. 299–316, 2008.

[9] M. Garcia, *Sedimentation Engineering*. American Society of Civil Engineers, 2008. [Online]. Available: http://ascelibrary.org/doi/abs/10.1061/9780784408148

[10] C. GOEURY and N. GOUTAL, "Analyse de sensibilité et propagation d'incertitude dans les modèles numériques : Application à l'hydraulique," 2014.

[11] A. Grass, "Sediment transport by waves and currents," SERC Cent. Mar. Tech., London, Tech. Rep. FL29, 1981.

[12] H. DELOUIS and P. CORDE, "Cours Fortran 95 - IDRIS," 2007.

[13] F. D. C. HAMMOND, A. D. HEATHERSHAW, and D. N. LANGHORNE, "A comparison between shields' threshold criterion and the movement of loosely packed gravel in a tidal channel," *Sedimentology*, vol. 31, no. 1, pp. 51–62, 1984. [Online]. Available: http://dx.doi.org/10.1111/j.1365-3091.1984.tb00722.x

[14] J. Hudson and P. K. Sweby, "Formulations for numerically approximating hyperbolic systems governing sediment transport," *Journal of Scientific Computing*, vol. 19, no. 1, pp. 225–252, Dec 2003. [Online]. Available: https://doi.org/10.1023/A:1025304008907

[15] ——, "A high-resolution scheme for the equations governing 2d bed-load sediment transport," *International Journal for Numerical Methods in Fluids*, vol. 47, no. 10-11, pp. 1085–1091, 2005. [Online]. Available: http://dx.doi.org/10.1002/fld.853

[16] R. P. Hunziker and M. N. R. Jaeggi, "Grain sorting processes," *Journal of Hydraulic Engineering*, vol. 128, no. 12, pp. 1060–1068, 2002.

[17] B. IOSS, "Revue sur l'analyse de sensibilité globale de modèles numériques," 2010.

[18] M. KADIRI-OTTMANI, "Traitement statistique d'un échantillon," *Technical report of CEA*, 2002.

[19] G. H. Keulegan, "Laws of turbulent flow in open channels," National Bureau of Standards, London, Tech. Rep. FL29, US.

[20] S. N. Lane, "Hydraulic modelling in hydrology and geomorphology: a review of high resolution approaches," *Hydrological Processes*, vol. 12, no. 8, pp. 1131–1150, 1998. [Online]. Available: http://dx.doi.org/10.1002/(SICI)1099-1085(19980630)12:8<1131::AID-HYP611>3.0.CO;2-K

[21] M. VAN ORMONDT, C. BRIERE, D.J.R. WALSTRA, L.C. VAN RIJN and A.M. TALMON, "FThe effects of bed slope and wave skewness on sediment transport and morphology," 2006.

[22] E. Meyer-Peter and R. Müller, "Formulas for bed-load transport," in *IAHSR 2nd meeting, Stockholm, appendix 2*. IAHR, 1948.

[23] J. Murillo and P. García-Navarro, "An exner-based coupled model for two-dimensional transient flow over erodible bed," *Journal of Computational Physics*, vol. 229, no. 23, pp. 8704 – 8732, 2010. [Online]. Available: http://www.sciencedirect.com/science/article/pii/S0021999110004432

[24] P. Nielsen, *Coastal bottom boundary layers and sediment transport*. World Scientific Publishing Co Inc, 1992, vol. 4.

[25] S. R., *Dynamics of marine sands*. H.R. Wallingford, 1997.

[26] R. ATA, C. GOEURY, P. LANG, J. DESOMBRE, J.M. HERVOUET, "TELEMAC MODELLING SYSTEM - Release 7.0 - USER MANUAL," 2014.

[27] A. Recking, "A comparison between flume and field bed load transport data and consequences for surface-based bed load transport prediction," *Water Resources Research*, vol. 46, no. 3, pp. n/a–n/a, 2010, w03518. [Online]. Available: http://dx.doi.org/10.1029/2009WR008007

[28] A. Siviglia, G. Stecca, D. Vanzo, G. Zolezzi, E. F. Toro, and M. Tubino, "Numerical modelling of two-dimensional morphodynamics with applications to river bars and bifurcations," *Advances in Water Resources*, vol. 52, pp. 243 – 260, 2013. [Online]. Available: http://www.sciencedirect.com/science/article/pii/S0309170812002928

[29] N. Struiksma, K. W. Olesen, C. Flokstra, and D. H. J. D. Vriend, "Bed deformation in curved alluvial channels," *Journal of Hydraulic Research*, vol. 23, no. 1, pp. 57–79, 1985. [Online]. Available: http://dx.doi.org/10.1080/00221688509499377

[30] A. Talmon, N. Struiksma, and M. Van Mierlo, "Laboratory measurements of the direction of sediment transport on transverse alluvial-bed slopes," *Journal of hydraulic research*, vol. 33, no. 4, pp. 495–517, 1995.

[31] P. TASSI and C. VILLARET, "SISYPHE USER'S MANUAL - Release 6.3 - USER MANUAL," 2014.

[32] L. L. Z. J. Vulliet, L., *Mécanique des sols et des roches (TGC volume 18): avec écoulements souterrains et transferts de chaleur*. PPUR Presses polytechniques, 2016, vol. TGC volume 18.

[33] W. WU, "Depth-averaged two-dimensional numerical modeling of unsteady flow and uniform sediment transport in open channels," *Journal of Hydraylic Engineering*, 2004.

[34] W. WU and S. WANG, "Formulas for sediment porosity and settling velocity," *Journal of Hydraylic Engineering*, 2006.

[35] B. A. . D. G. Yossef, M. F., *Modelling large scale and long term morphological response to engineering interventions at river bifurcation*, G. Constantinescu, M. Garcia, and D. Hanes, Eds. River Flow 2016: Iowa City, USA: Crc Press, July 11-14 2016.